Biophysical Journal, Volume *120*

Supplemental information

Phase separation of the LINE-1 ORF1 protein is mediated by the N-terminus and coiled-coil domain

Jocelyn C. Newton, Mandar T. Naik, Grace Y. Li, Eileen L. Murphy, Nicolas L. Fawzi, John M. Sedivy, and Gerwald Jogl

Table S1. Nucleotide and Protein Sequences of Human LINE-1 ORF1$_{1\text{-}338}$ (UniProt Q9UN81)
The nucleotide sequence was codon optimized for expression in *E. coli* and subcloned into pET26b using NdeI and XhoI (cut sites italicized in the nucleotide sequence).

E. coli codon optimized ORF1 gene sequence used in this study

*CAT*ATGGGTAAAAAACAGAATCGTAAGACCGGTAACAGCAAAA
CCCAAAGCGCGAGCCCGCCGCCGAAGGAACGCAGCAGCAGCCCGG
CGACCGAGCAGAGCTGGATGGAAAACGACTTCGATGAGCTGCGTG
AGGAAGGTTTTCGTCGTAGCAACTACAGCGAGCTGCGTGAAGACA
TCCAAACCAAGGGCAAAGAGGTGGAAAACTTTGAAAAGAACCTGG
AGGAATGCATCACCCGTATTACCAACACCGAGAAGTGCCTGAAAG
AGCTGATGGAACTGAAGACCAAAGCGCGTGAACTGCGTGAGGAAT
GCCGTAGCCTGCGTAGCCGTTGCGACCAGCTGGAGGAACGTGTGA
GCGCGATGGAGGATGAAATGAACGAGATGAAGCGTGAGGGTAAAT
TCCGTGAGAAGCGTATCAAACGTAACGAACAGAGCCTGCAAGAGA
TTTGGGATTACGTTAAGCGTCCGAACCTGCGTCTGATCGGTGTGC
CGGAGAGCGACGTTGAAAACGGCACCAAACTGGAAAACACCCTGC
AGGATATCATTCAAGAGAACTTTCCGAACCTGGCGCGTCAAGCGA
ACGTGCAGATCCAAGAAATTCAGCGTACCCCGCAACGTTATAGCA
GCCGTCGTGCGACCCCGCGTCACATCATTGTGCGTTTCACCAAGG
TTGAGATGAAGGAAAAAATGCTGCGTGCGGCGCGTGAGAAAGGTC
GTGTTACCCTGAAGGGCAAACCGATTCGTCTGACCGCGGATCTGA
GCGCGGAAACCCTGCAGGCGCGTCGTGAGTGGGGTCCGATCTTCA
ACATTCTGAAGGAGAAGAACTTTCAACCGCGTATCAGCTACCCGG
CGAAACTGAGCTTCATTAGCGAGGGCGAAATCAAGTACTTCATCG
ACAAGCAGATGCTGCGTGATTTCGTTACCACCCGTCCGGCGCTGA
AGGAGCTGCTGAAAGAAGCGCTGAATATGGAACGCAATAACCGCT
ACCAACCGCTGCAAAATCACGCGAAAATGTAA*CTCGAG*

Protein Sequence of ORF1$_{1\text{-}338}$ used in this study

MGKKQNRKTGNSKTQSASPPPKERSSSPATEQSWMENDFDELREEGFRRSNYSELREDIQTKGKEVENFE
KNLEECITRITNTEKCLKELMELKTKARELREECRSLRSRCDQLEERVSAMEDEMNEMKREGKFREKRIK
RNEQSLQEIWDYVKRPNLRLIGVPESDVENGTKLENTLQDIIQENFPNLARQANVQIQEIQRTPQRYSSR
RATPRHIIVRFTKVEMKEKMLRAAREKGRVTLKGKPIRLTADLSAETLQARREWGPIFNILKEKNFQPRI
SYPAKLSFISEGEIKYFIDKQMLRDFVTTRPALKELLKEALNMERNNRYQPLQNHAKMLEHHHHHH

Table S2. Concentration measurements of the dilute phase of ORF1.
Concentrations in μM of ORF1 measured in the dilute phase of the assays plotted in the main text Figures 3G and 4B.

ORF1 Construct	150 mM NaCl	200 mM NaCl	250 mM NaCl	300 mM NaCl	350 mM NaCl	400 mM NaCl	450 mM NaCl	500 mM NaCl
$ORF1_{1\text{-}338}$	9 ± 1	22 ± 1	76 ± 4	220 ± 10	311 ± 10	308 ± 11	305 ± 10	293 ± 8
$ORF1_{66\text{-}338}$	234 ± 24	324 ± 6	335 ± 7	340 ± 3	339 ± 4	332 ± 8	340 ± 3	335 ± 7
$ORF1_{1\text{-}131}$	340 ± 32	319 ± 9	314 ± 34	31 ± 5	337 ± 28	322 ± 2	318 ± 8	326 ± 1
$ORF1_{1\text{-}141}$	77 ± 7	130 ± 9	255 ± 5	323 ± 10	317 ± 7	311 ± 20	319 ± 1	323 ± 2
$ORF1_{1\text{-}338}$ L93P	4 ± 2	8 ± 0.4	33 ± 2	115 ± 3	288 ± 11	294 ± 5	308 ± 29	323 ± 15
$ORF1_{1\text{-}338}$ S27D	4 ± 1	10 ± 2	30 ± 3	152 ± 15	301 ± 4	304 ± 2	300 ± 4	293 ± 16
$ORF_{1\text{-}338}$ K3A/K4A	6 ± 1	17 ± 5	61 ± 16	190 ± 38	293 ± 31	298 ± 24	297 ± 34	296 ± 31
$ORF_{1\text{-}338}$ K3E/K4E	13 ± 2	35 ± 1	119 ± 9	323 ± 10	316 ± 2	320 ± 7	320 ± 0.3	316 ± 4
$ORF_{1\text{-}338}$ R7E/K8E	11 ± 2	42 ± 9	147 ± 17	303 ± 6	274 ± 22	276 ± 25	265 ± 21	277 ± 9
$ORF_{1\text{-}338}$ K3A/K4A/ R7A/K8A	11 ± 3	40 ± 4	133 ± 10	278 ± 20	293 ± 21	258 ± 21	277 ± 39	313 ± 6
$ORF_{1\text{-}338}$ K3E/K4E/ R7E/K8E	11 ± 2	37 ± 2	133 ± 5	316 ± 1	312 ± 3	316 ± 3	316 ± 2	315 ± 2

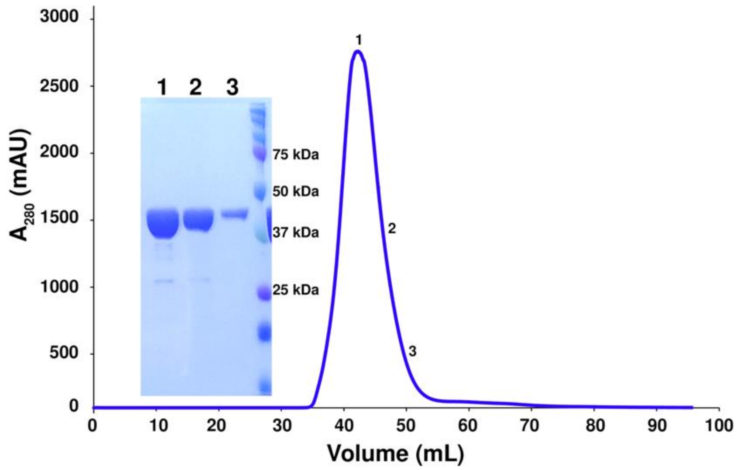

Figure S1. Gel Filtration Profile of ORF1$_{1-338}$.
ORF1$_{1-338}$ elutes as a trimer on a Hi-Prep 16/60 Sephacryl S300 in 20 mM Tris pH8.0, 1 M NaCl, 1 mM DTT with little evidence of hexamers or higher order oligomers.

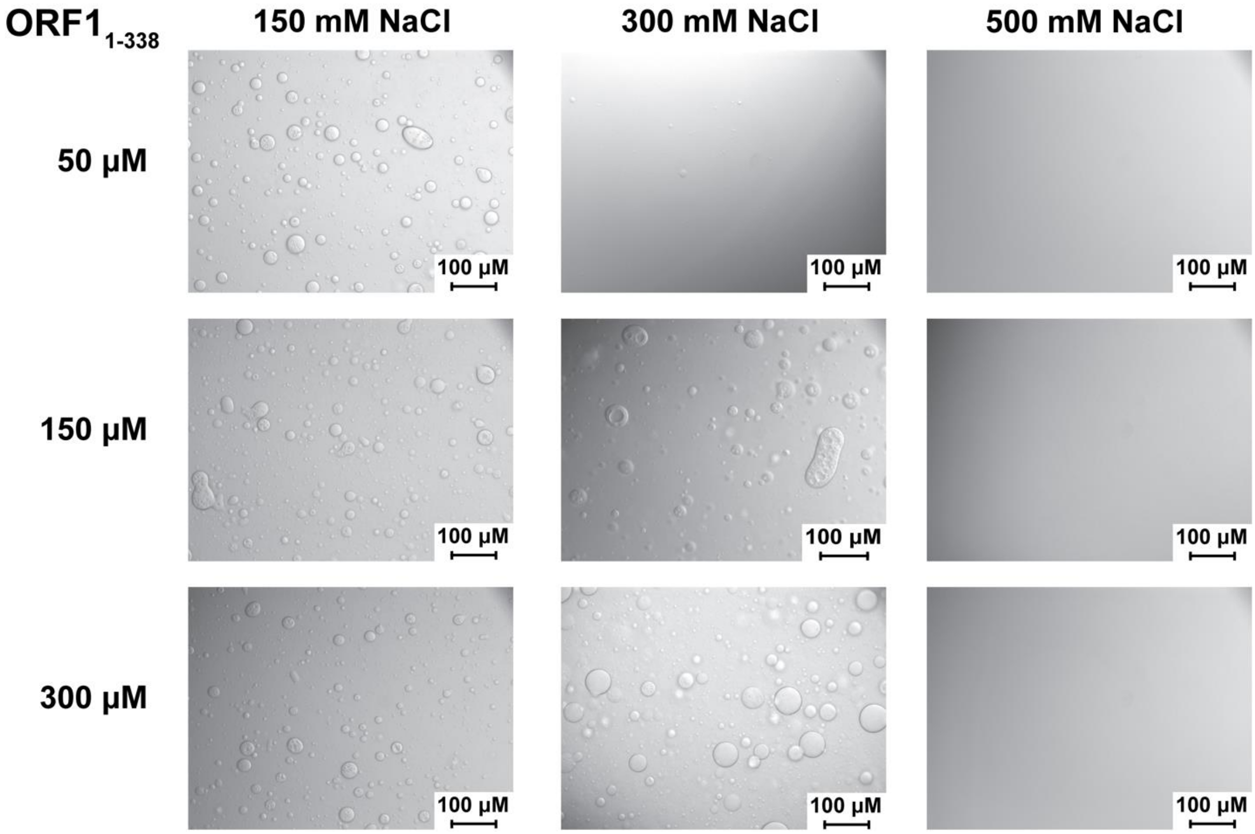

Figure S2. ORF1$_{1\text{-}338}$ phase separation is dependent on protein and salt concentration. At lower NaCl concentrations, ORF1$_{1\text{-}338}$ phase separates more readily than at higher NaCl concentrations. This phenomenon is dependent on both the protein concentration and salt concentration. Images collected at room temperature with noted concentration of ORF1$_{1\text{-}338}$ in 20 mM Tris pH 8.0, 1 mM DTT and the NaCl concentration listed.

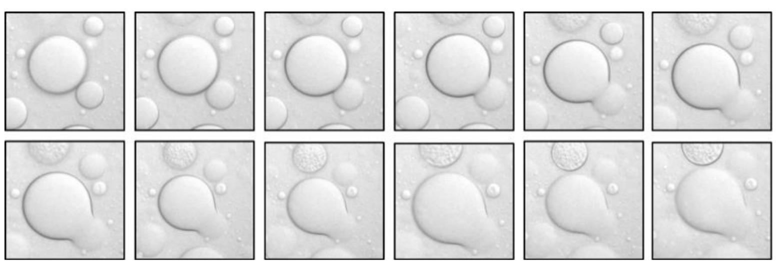

Figure S3. ORF1 droplets behave as liquids.
Images were taken in succession (within approximately 10 seconds) to demonstrate that the ORF1 droplets are capable of flowing and fusing in solution.

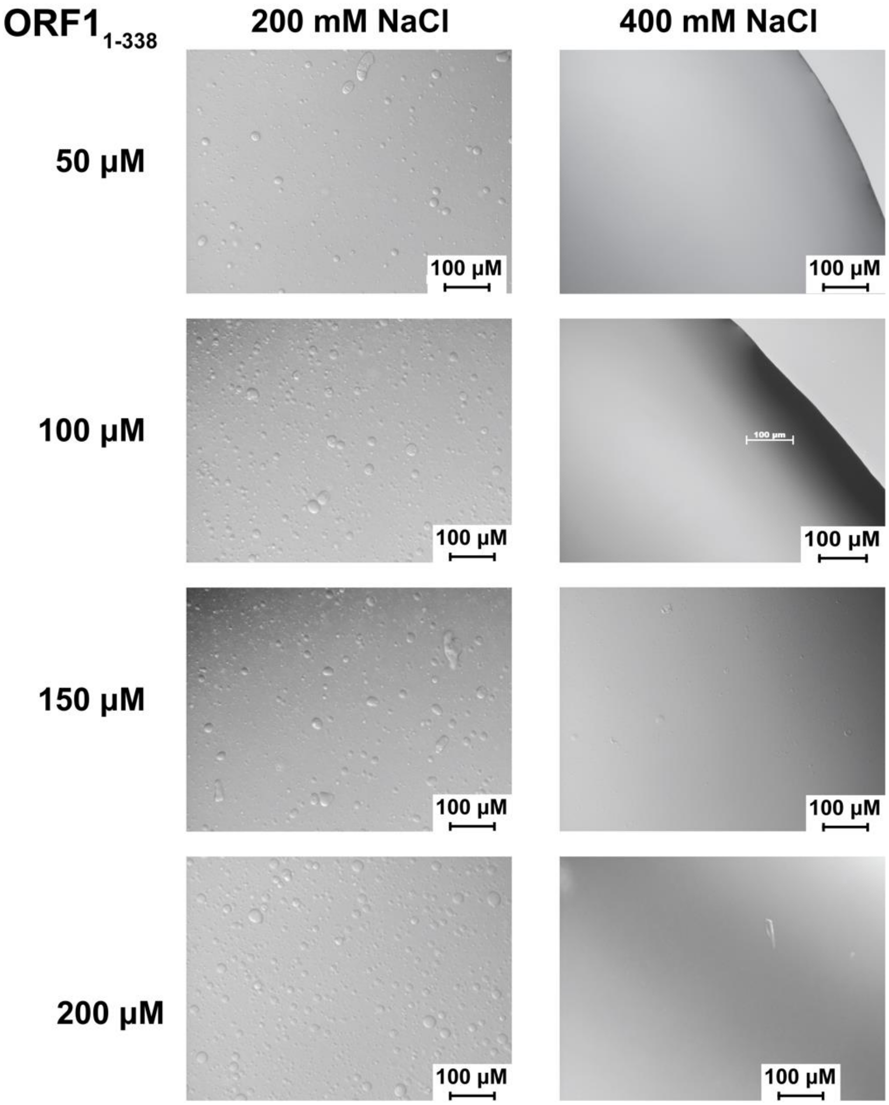

Figure S4. $ORF1_{1\text{-}338}$ phase separation at 200 and 400 mM NaCl.
At higher protein concentrations, some amorphous aggregates or hydrogels can be observed in the 200 mM NaCl conditions as well as low levels of phase separation in the 400 mM NaCl conditions.

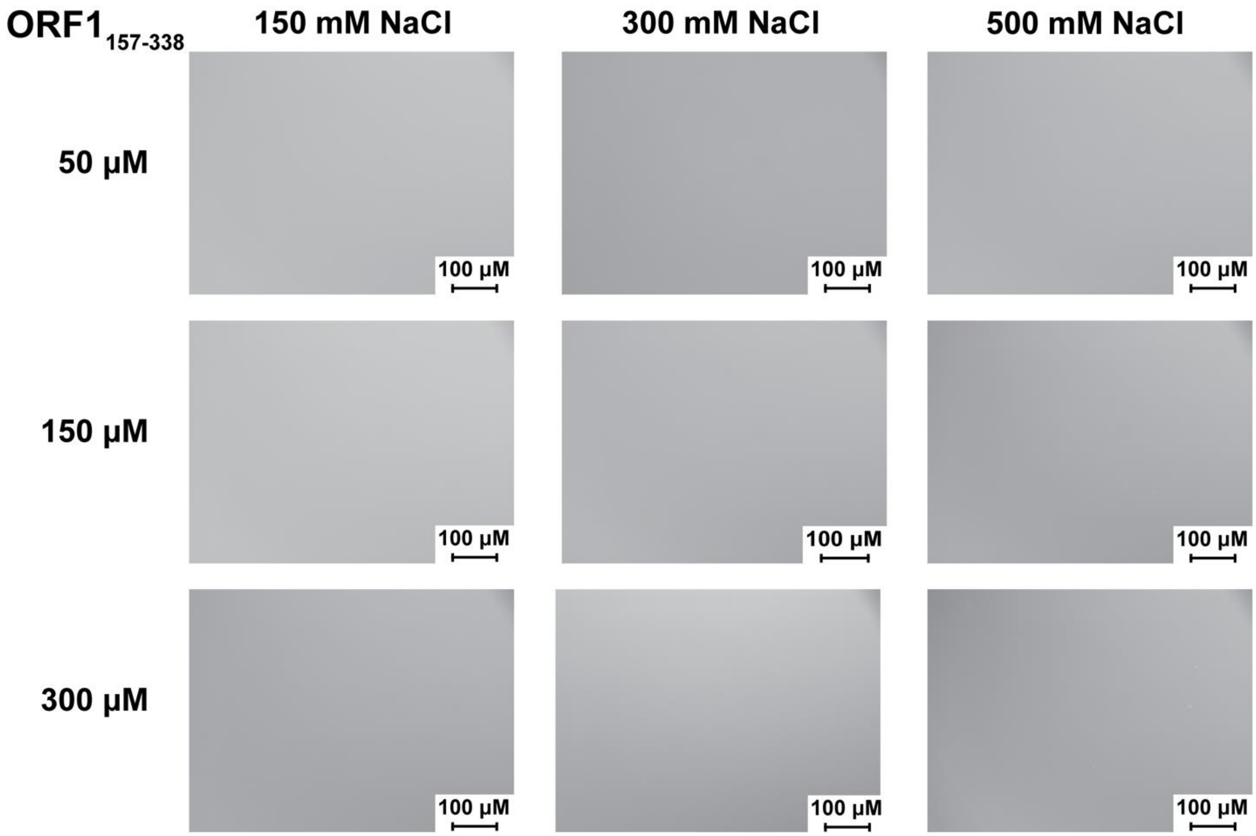

Figure S5. The RRM and CTD domains do not contribute to ORF1 phase separation. ORF1$_{157\text{-}338}$ does not phase-separate in any condition tested. Images were collected with noted concentrations of ORF1$_{157\text{-}338}$ at room temperature in 20 mM Tris pH 8.0 and 1 mM DTT with NaCl concentration listed.

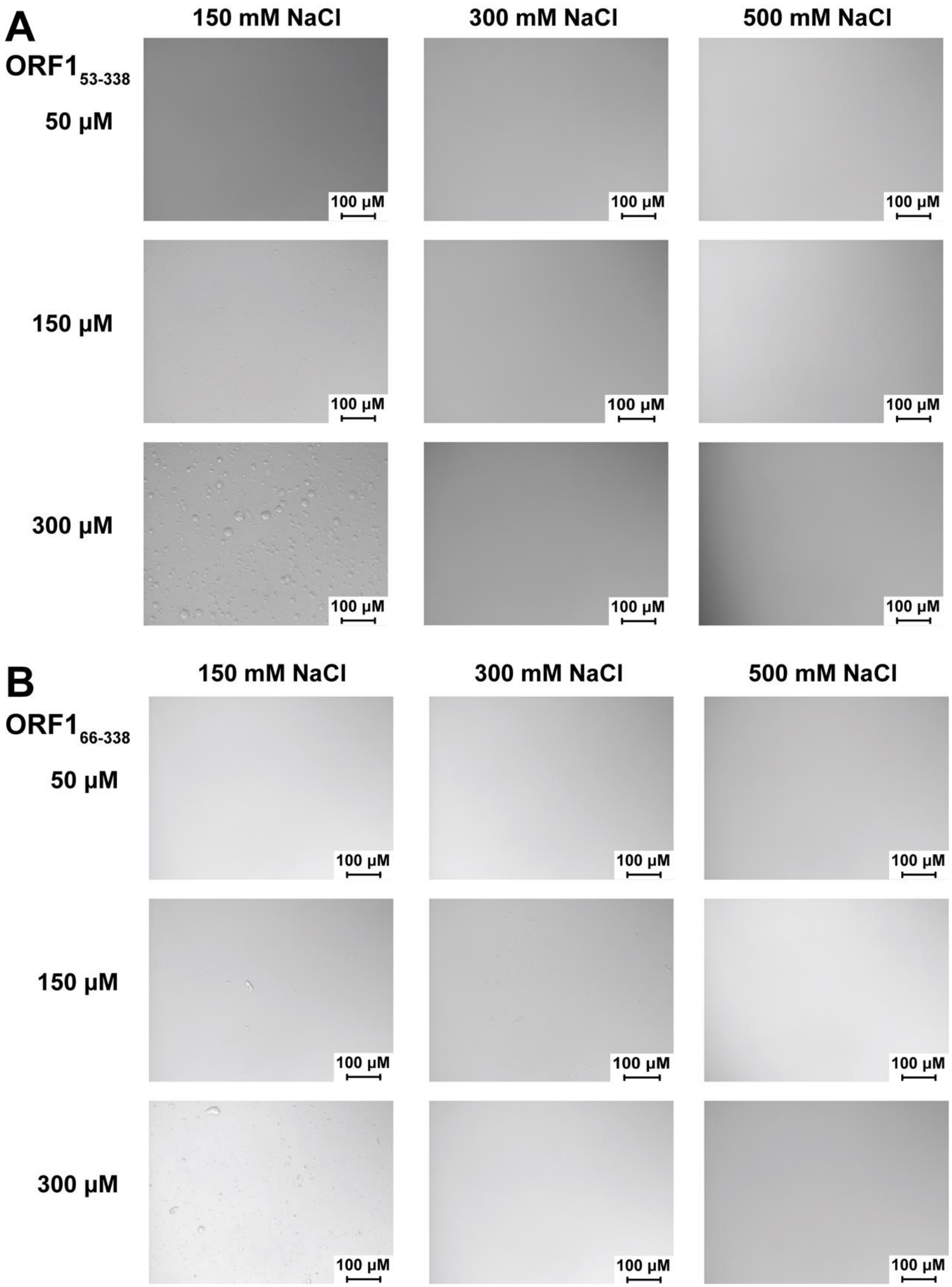

Figure S6. Truncation of the disordered N-terminus reduces ORF1 phase separation. Truncation of the ORF1 N-terminus at residues 52 (**A**) or 65 (**B**) reduces ORF1 phase separation but does not abolish phase separation in the lowest NaCl concentrations tested. Images were collected with noted concentration of $ORF1_{52\text{-}338}$ or $ORF1_{66\text{-}338}$ at room temperature in 20 mM Tris pH 8.0, 1 mM DTT with NaCl concentration listed.

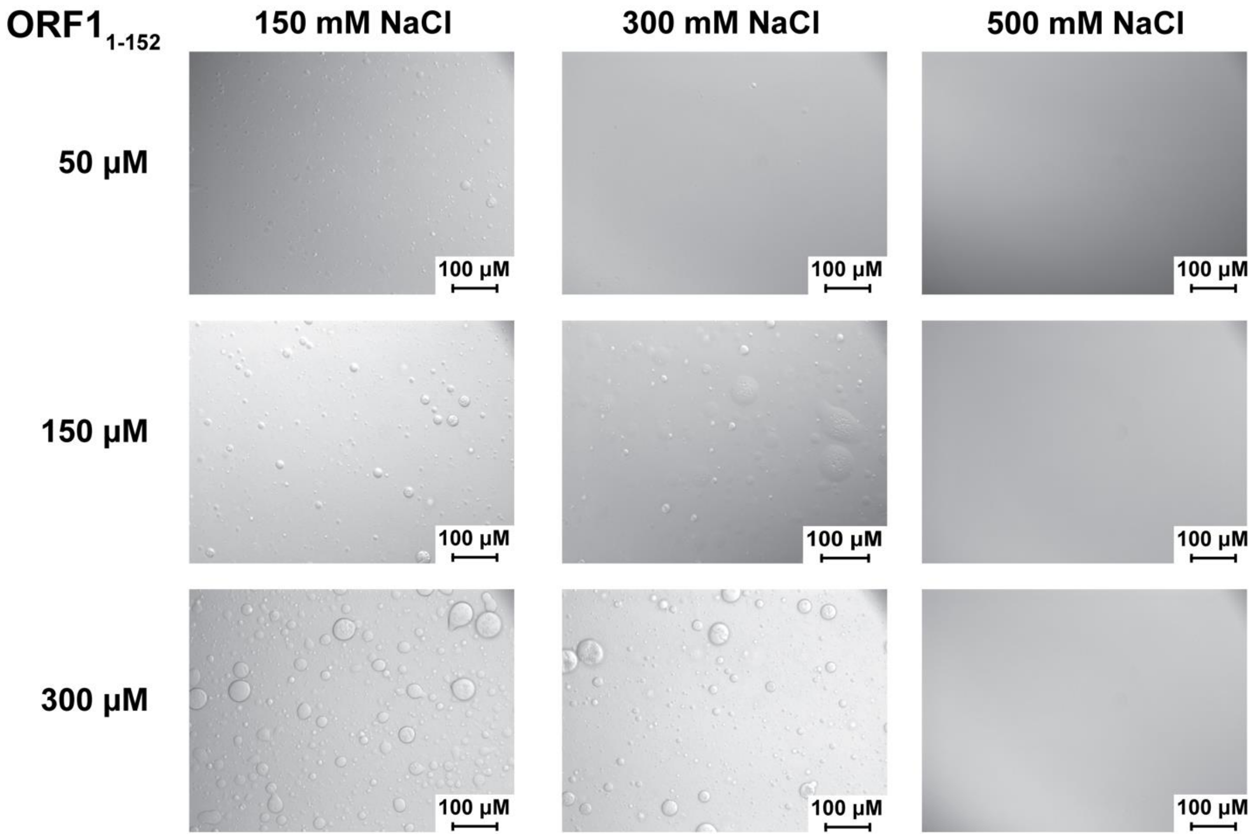

Figure S7. A minimal construct of the N-terminus and coiled coil domain retains the ability to phase separate.
The $ORF1_{1\text{-}152}$ construct contains both the disordered N-terminus and coiled coil domains and is capable of phase separating in conditions similar to that of the full-length $ORF_{1\text{-}338}$ protein. Images were collected with noted concentration of $ORF1_{1\text{-}152}$ at room temperature in 20 mM Tris pH 8.0, 1 mM DTT with NaCl concentration listed.

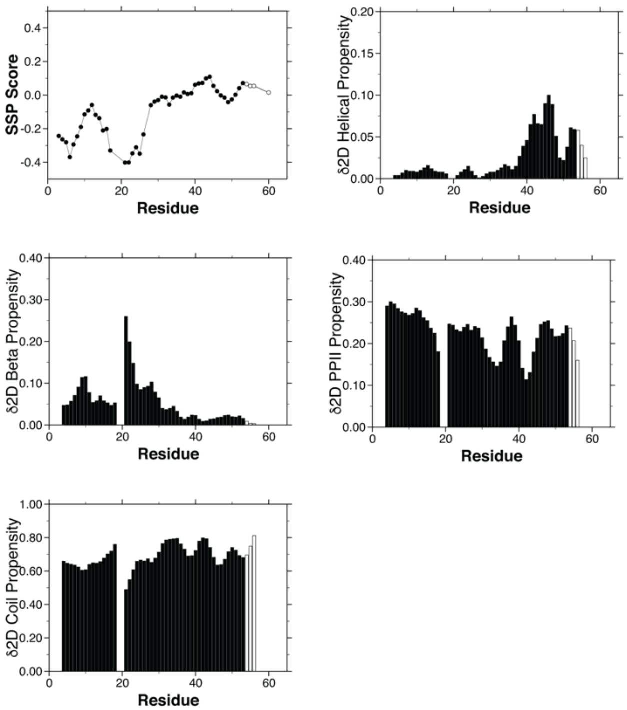

Figure S8. Additional NMR Data

The secondary structure propensity (SSP) score and δ2D Helical Propensity, δ2D Beta Propensity, δ2D PPII Propensity, and δ2D Coil Propensity scores show that residues 41-49 have slight α-helical character. Open circles and open bars correspond to residues from the histidine tag.

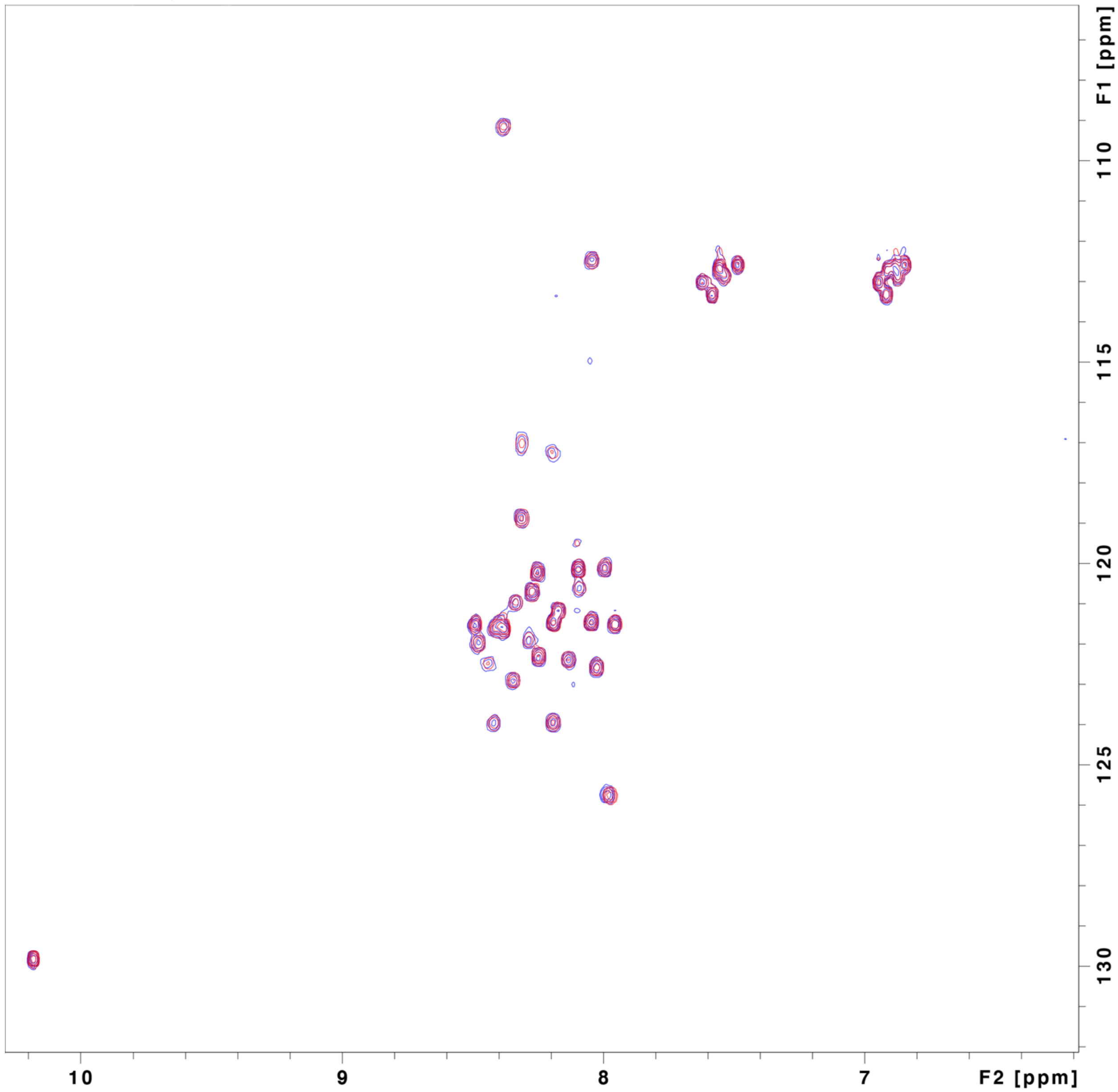

Figure S9. No chemical shift perturbations are observed with increasing concentrations of ORF1$_{1\text{-}53}$.
ORF1$_{1\text{-}53}$ is shown at 20 μM (blue) and 1 mM (red) concentration in 200 mM NaCl and 20 mM HEPES at pH 7.25 at 25 °C.

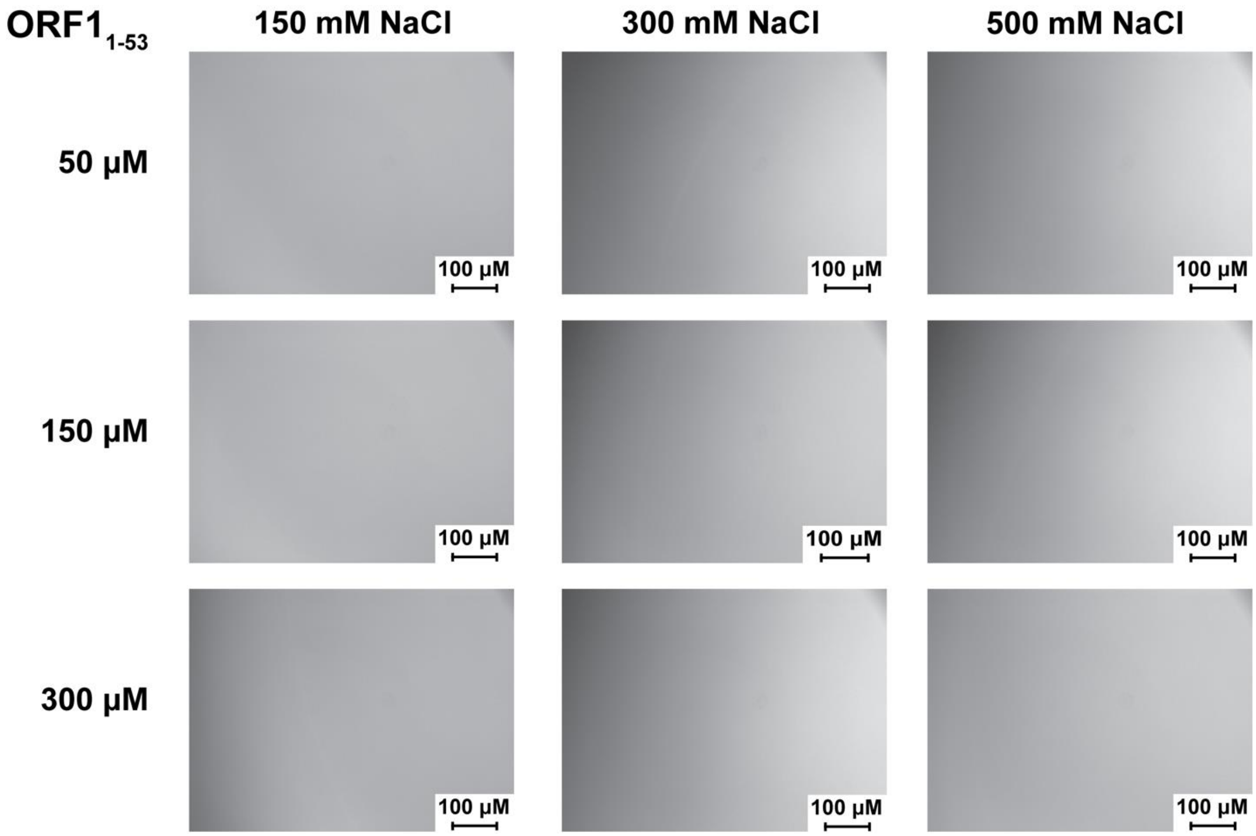

Figure S10. ORF1$_{1\text{-}53}$ is not sufficient for phase separation.
ORF1$_{1\text{-}53}$ does not phase separate in any condition tested by DIC microscopy. Images were collected with noted concentration of ORF1$_{1\text{-}53}$ at room temperature in 20 mM Tris pH 8.0, 1 mM DTT with NaCl concentration listed.

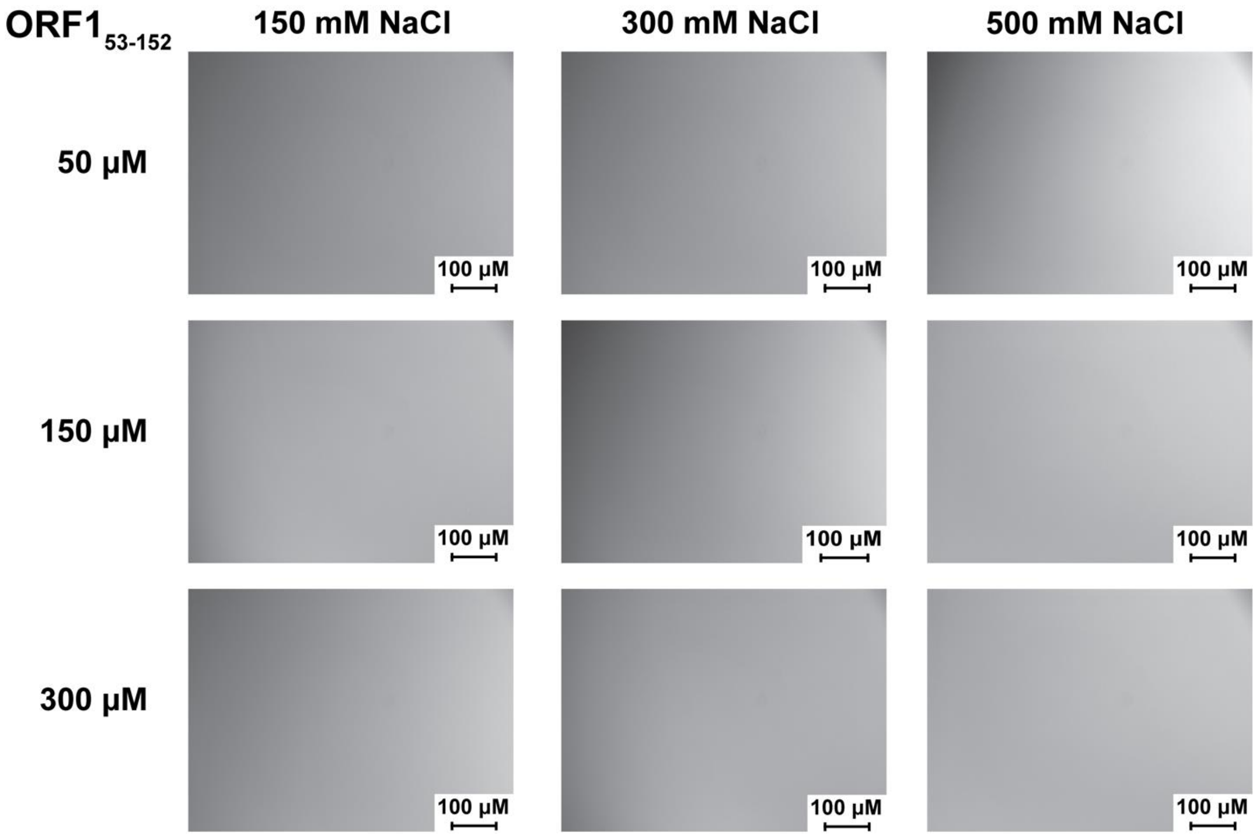

Figure S11. The ORF1 coiled-coil domain is not sufficient for phase separation.
ORF1$_{53-152}$ isolates the coiled-coil domain and does not phase separate in any condition tested. Images were collected with noted concentration of ORF1$_{53-152}$ at room temperature in 20 mM Tris pH 8.0, 1 mM DTT with NaCl concentration listed.

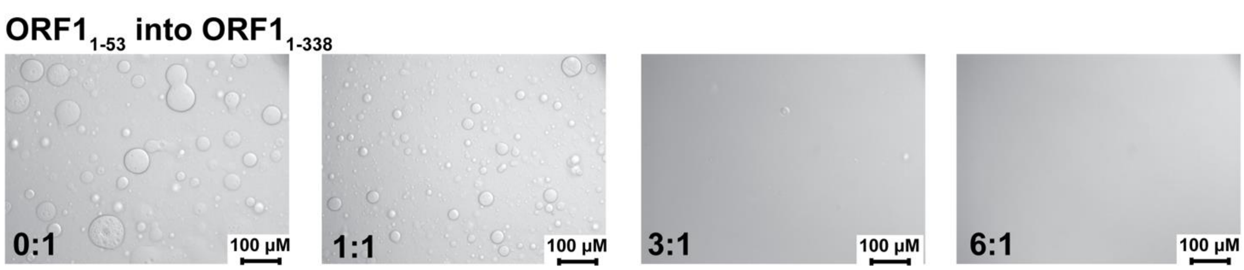

Figure S12. Titration of ORF1$_{1-53}$ into ORF1$_{1-338}$ disrupts phase separation in a concentration dependent manner.
Increasing the concentration of ORF1$_{1-53}$ disrupts phase separation of full-length ORF1$_{1-338}$ in a concentration dependent manner. Ratios in the image panels describe the molar ratio of ORF1$_{1-53}$:ORF1$_{1-338}$. Images were collected with 300 μM ORF1$_{1-338}$ at room temperature in 20 mM Tris pH 8.0, 300 mM NaCl, 1 mM DTT with increasing concentrations of ORF1$_{1-53}$ as indicated by the molar ratio in the figure panels.

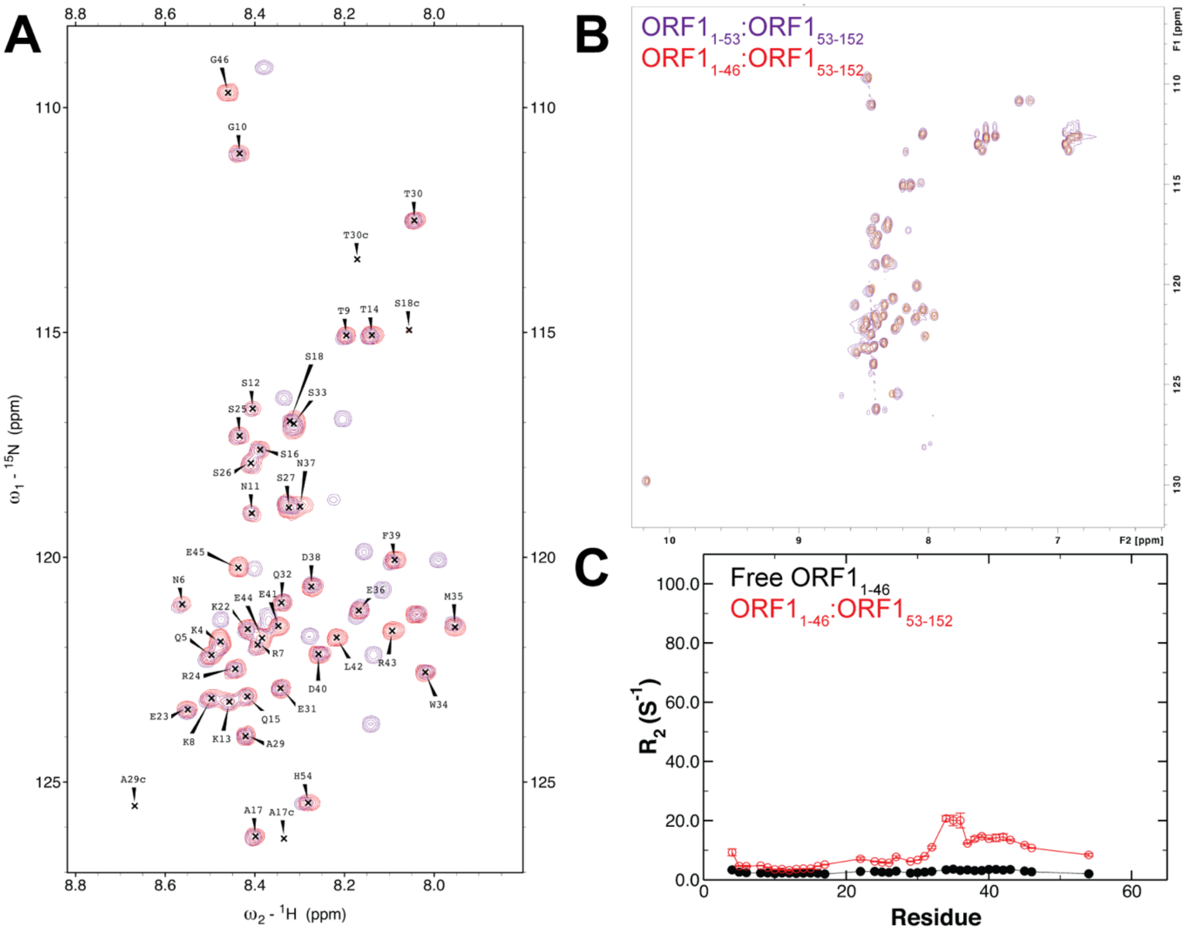

Figure S13. ORF1$_{1\text{-}46}$ remains disordered but cannot interact with ORF1$_{53\text{-}152}$.
A. The ^{15}N-^{1}H HSQC correlation spectra overlay nicely between ORF1$_{1\text{-}53}$ (purple) and ORF1$_{1\text{-}46}$ (red). **B.** ORF1$_{1\text{-}46}$ no longer displays significant line broadening in the presence of ORF1$_{53\text{-}152}$ (red) as observed with ORF1$_{1\text{-}53}$ (purple), indicating that the interaction is disrupted by removing residues 47-53. **C.** The values of R_2 are slightly elevated in ORF1$_{1\text{-}46}$ in the presence of ORF1$_{53\text{-}152}$ (red) compared to free ORF1$_{1\text{-}46}$ (black), unlike the highly elevated values observed for ORF1$_{1\text{-}53}$ in the presence of ORF1$_{53\text{-}152}$. Open circles correspond to residues from the histidine tag. These data were acquired at 700 μM ORF1$_{1\text{-}53}$ or ORF1$_{1\text{-}46}$ and their respective 1:1 molar ratio complexes with 700 μM ORF1$_{53\text{-}152}$ (red).

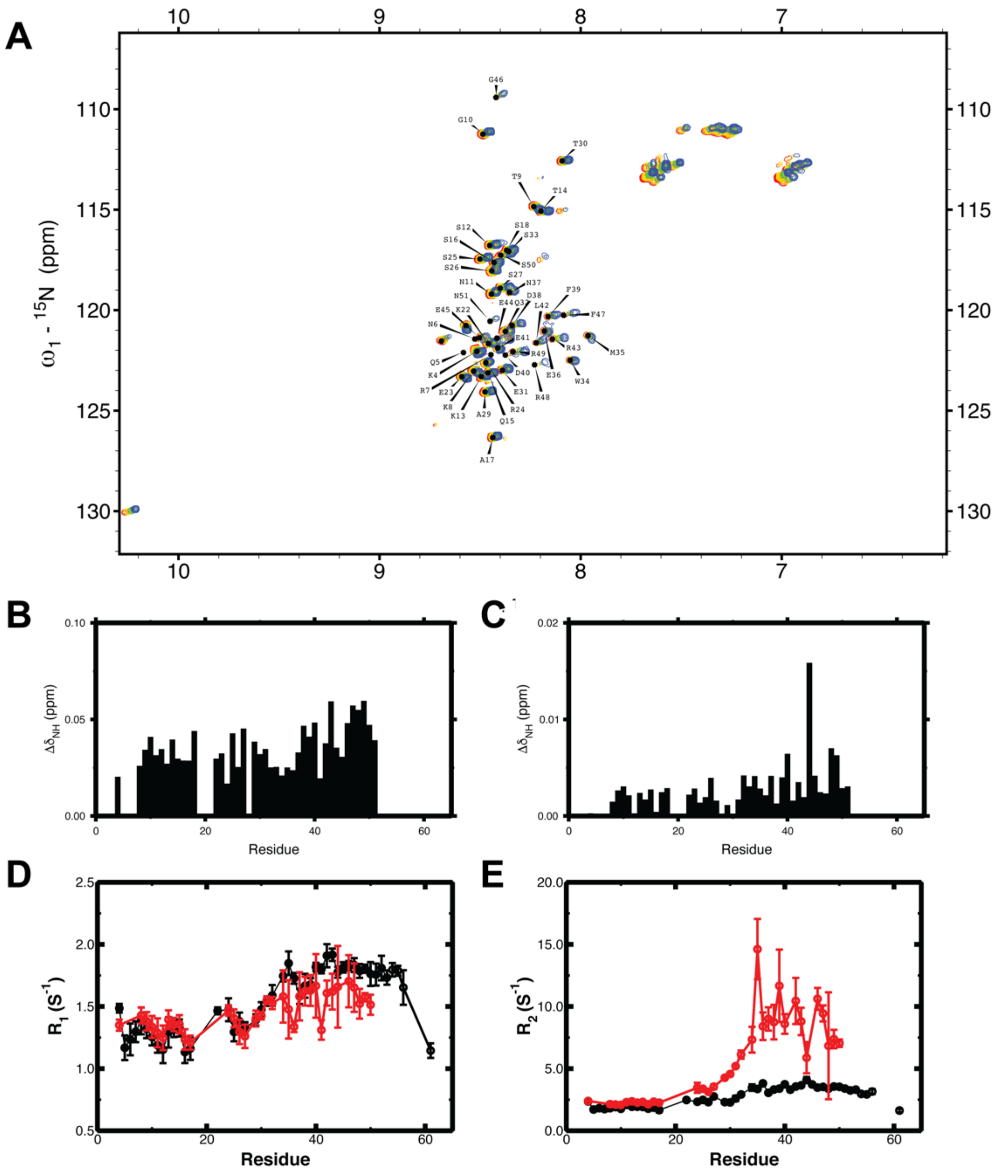

Figure S14. NMR Characterization of the disordered N-terminal region of ORF1$_{1\text{-}152}$ at varying salt concentrations and protein concentrations.

A. The ^{15}N-^{1}H HSQC correlation spectra of ^{15}N labeled ORF1$_{1\text{-}152}$ in 20 mM MES pH 6.0, 1 mM DTT, 7% D_2O at 400 mM (blue), 600 mM (green), 800 mM (yellow), and 933 mM (red) NaCl (collected in 3 mm NMR tubes to avoid issues with long pulse lengths in high salt conditions) are similar, showing no qualitative changes in the spectra arising from additional interactions. Only the disordered N-terminal region until about residue 50 is visible. We note that samples were all initially created at 200 μM ORF1$_{1\text{-}152}$. At 100 mM and 200 mM NaCl measurements were attempted but there remained no observable protein by spectrophotometry after clearing the supernatant. At higher salt, 17 μM remained at 400 mM NaCl, 67 μM at 600 mM, while no apparent phase separation occurred and approximately 200 μM remained after centrifugation at both 800 mM and 933 mM NaCl. **B.** Chemical shift differences between 400 mM and 933 mM NaCl for ORF1$_{1\text{-}152}$ indicate to significant regional difference, suggesting we cannot directly observe the contacts using this approach in the dispersed phase samples. **D.** Chemical shift differences for ORF1$_{1\text{-}152}$ at 600 mM NaCl between 67 μM (near the saturation concentration) and 33 μM (below the saturation concentration) are small and uniform, suggesting again that this approach cannot observe interactions leading to phase separation. **D.** R_1 and **E.** R_2 for 179 μM (below saturation concentration) ORF1$_{1\text{-}152}$ at 933 mM NaCl shown in red compared to ORF1$_{1\text{-}53}$ acquired at 700 μM protein and 200 mM NaCl shown in black. (Heteronuclear NOE was attempted but the signal to noise ratio in 3 mm tubes for weak peaks was prohibitive.) R_2 is enhanced in the region of residues 35-50 in ORF1$_{1\text{-}152}$ with only small change in R_1. This elevated R_2 suggests some interaction at this site within the trimeric ORF1$_{1\text{-}152}$ assembly, mirroring what we observed mixing ORF$_{1\text{-}53}$ with ORF1$_{53\text{-}152}$. The lack of large chemical shifts compared to the disordered 1-53 and the small change in R_1 do not support a large structural change. The uniformity of the values across this region suggests the elevation is more than can be explained by simple tethering of the region to the coiled-coil trimer.

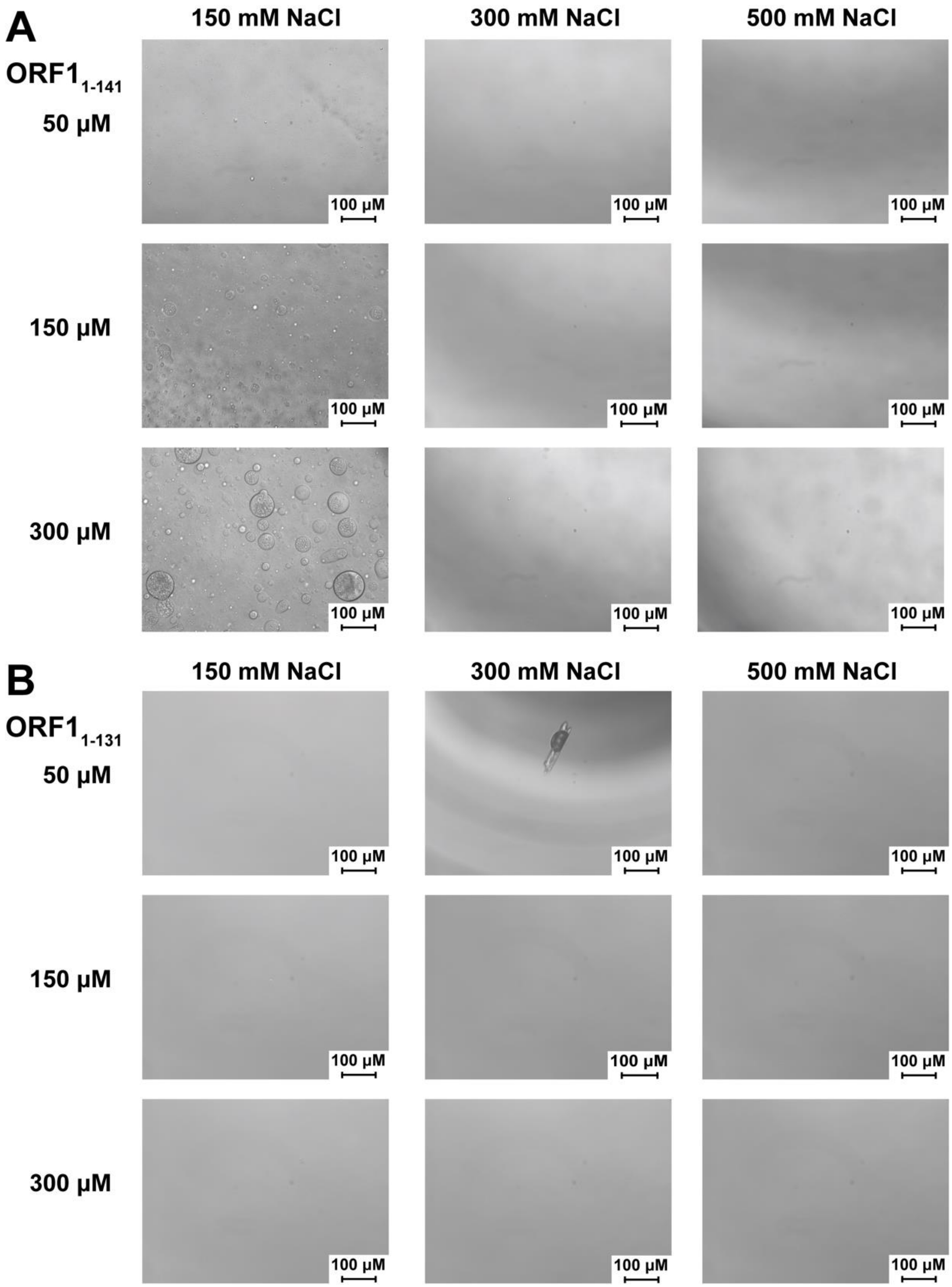

Figure S15. Truncation of the C-terminus of the coiled-coil domain disrupts ORF1 phase separation.

Truncation of the C-terminus of the coiled-coil domain at residues 141 (**A.**) or 131 (**B.**) reduces ORF1 phase separation but does not abolish phase separation in the $ORF1_{1-141}$ construct. Images were collected with noted concentration of $ORF1_{1-141}$ or $ORF1_{1-131}$ at room temperature in 20 mM Tris pH 8.0, 1 mM DTT with NaCl concentration listed.

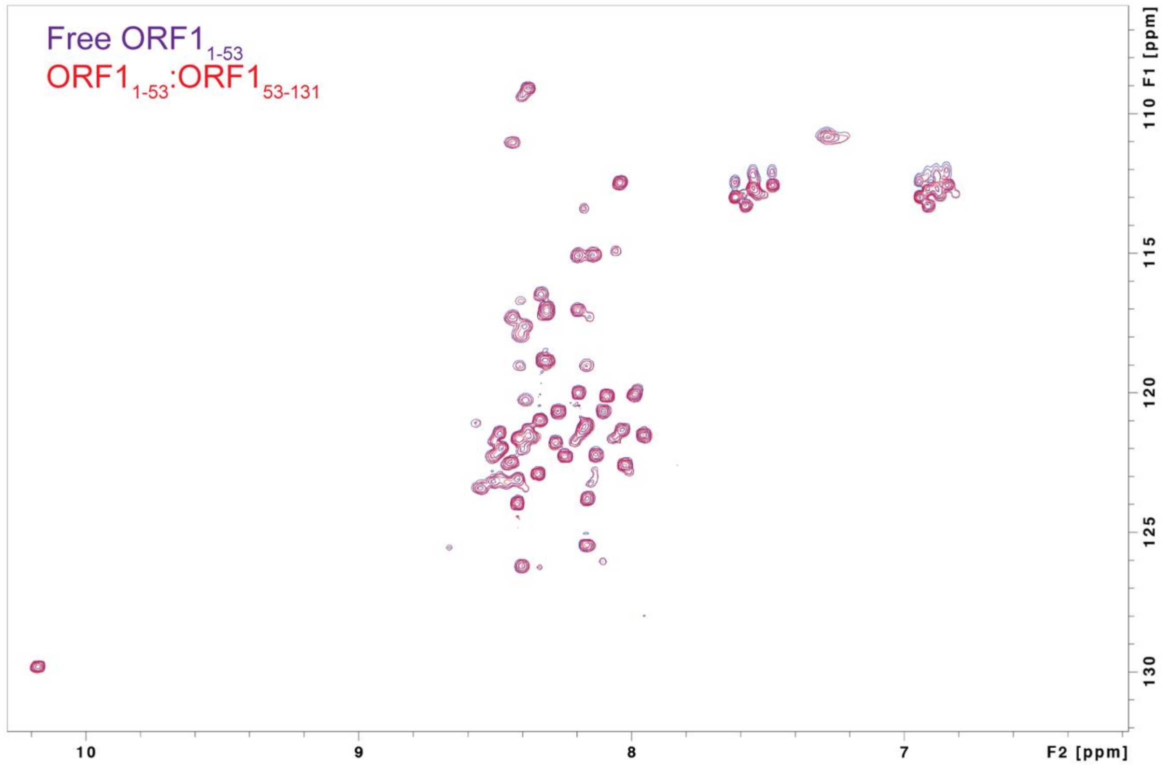

Figure S16. ORF1$_{1-53}$ cannot bind to the C-terminal portion of the coiled-coil domain after truncating residues 132-152.

No differences are observed between the ^{15}N-^{1}H HSQC correlation spectra of free ORF1$_{1-53}$ (790 μM) and ORF1$_{1-53}$ (300 μM) in the presence of the ORF1$_{53-131}$ (300 μM) truncated coiled-coil domain, demonstrating that the C-terminal 22 residues are necessary for that interaction.

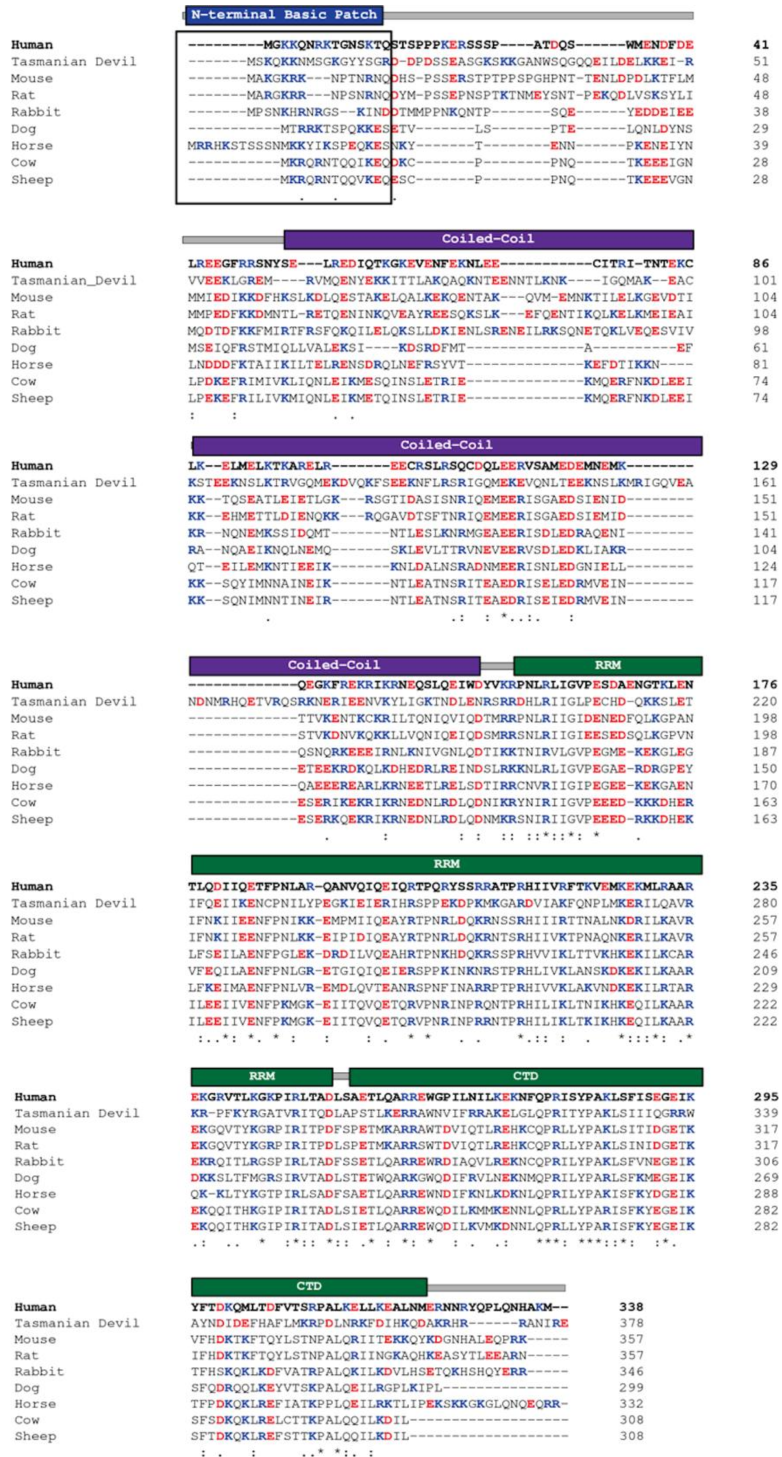

Figure S17. The basic residues at the N-terminus of ORF1 are highly conserved.
Accession numbers for the sequences are as follows: Human, AAA36590.1; Mouse, P11260.2; Tasmanian Devil, NW 003849619.1; Rat, AAY88219.1. The remaining sequences were obtained from L1Base2 (1). Domain architecture placed above the alignments corresponds to the human ORF1 domain boundaries.

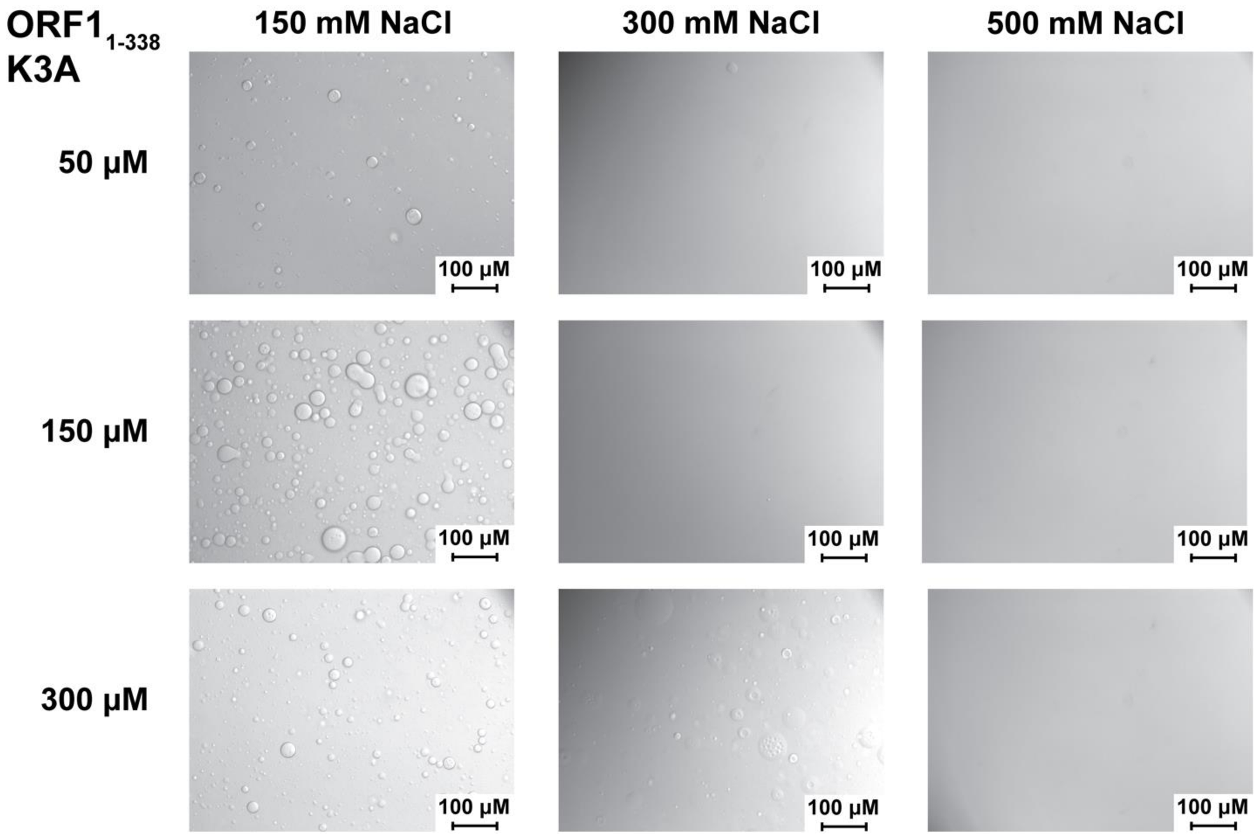

Figure S18. Phase separation of ORF1$_{1\text{-}338}$ K3A.
Mutations in the disordered N-terminal region alter the behavior of ORF1 phase separation. Images were collected with noted concentration of ORF1$_{1\text{-}338}$ K3A at room temperature in 20 mM Tris pH 8.0, 1 mM DTT with NaCl concentration listed.

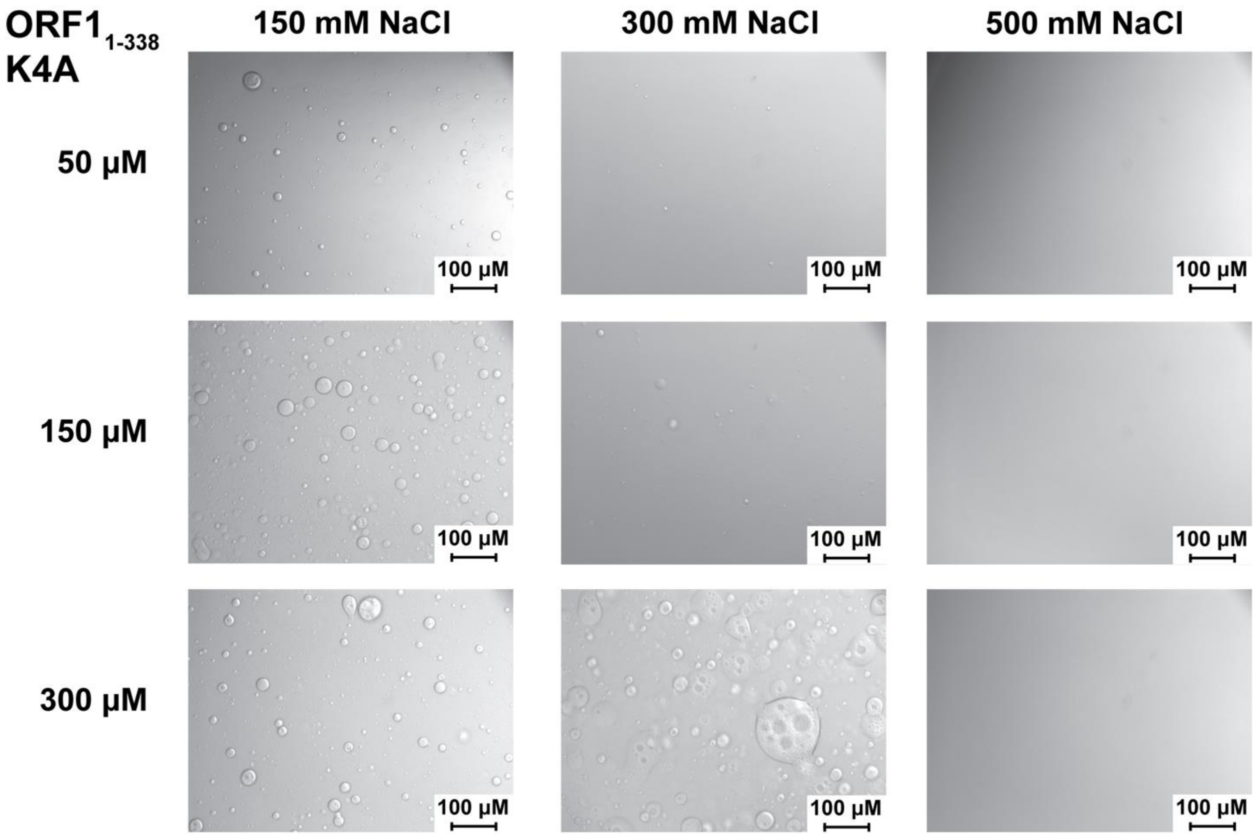

Figure S19. Phase separation of ORF1$_{1\text{-}338}$ K4A.
Mutations in the disordered N-terminal region alter the behavior of ORF1 phase separation. Images were collected with noted concentration of ORF1$_{1\text{-}338}$ K4A at room temperature in 20 mM Tris pH 8.0, 1 mM DTT with NaCl concentration listed.

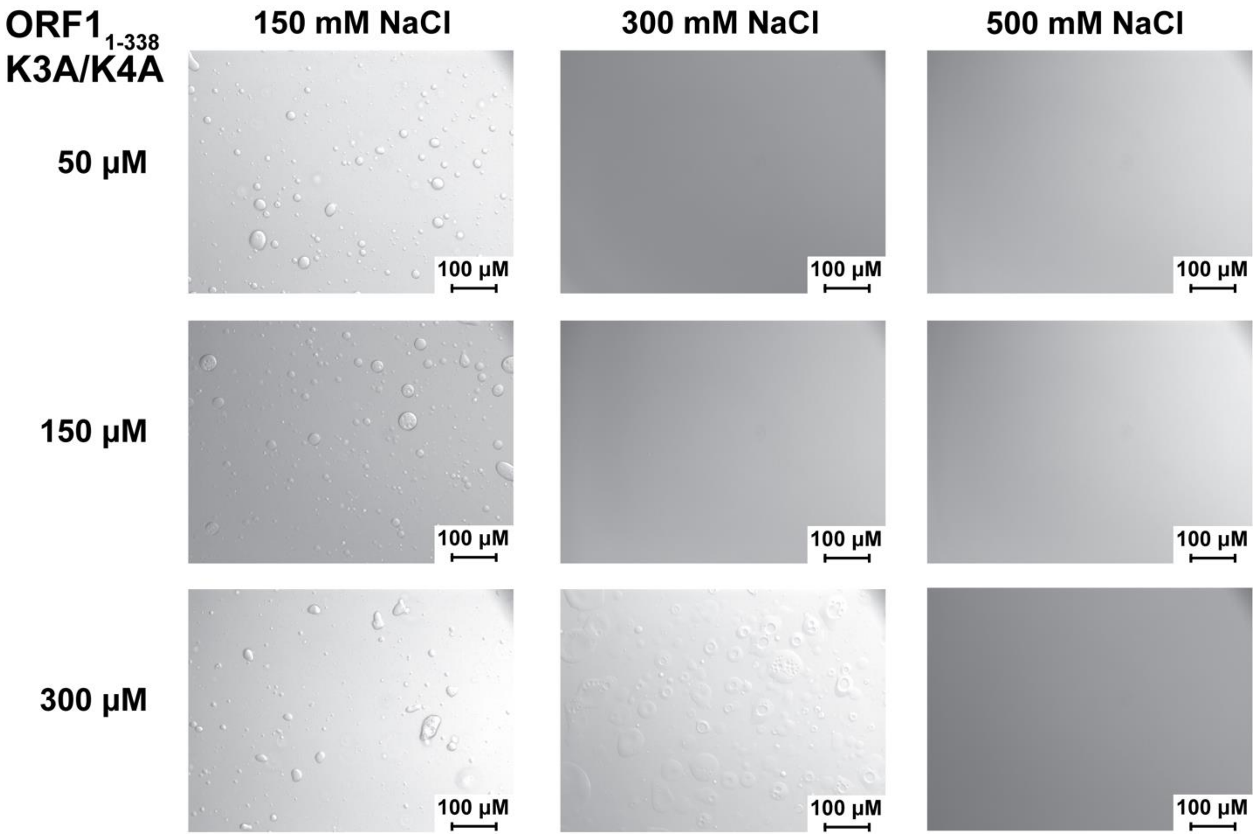

Figure S20. Phase separation of ORF1$_{1\text{-}338}$ K3A/K4A.
Mutations in the disordered N-terminal region alter the behavior of ORF1 phase separation. Images were collected with noted concentration of ORF1$_{1\text{-}338}$ K3A/K4A at room temperature in 20 mM Tris pH 8.0, 1 mM DTT with NaCl concentration listed.

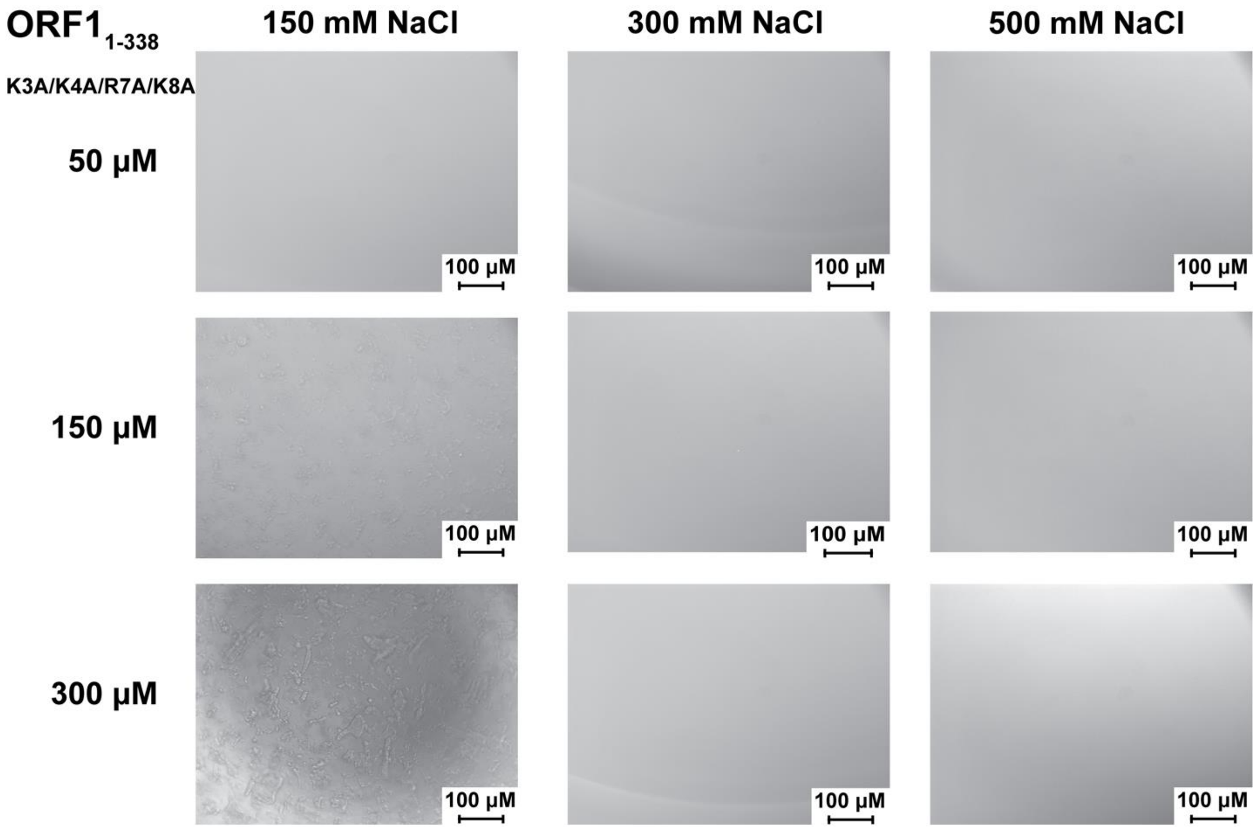

Figure S21. Phase separation of ORF1$_{1\text{-}338}$ K3A/K4A/R7A/K8A.
Mutations in the disordered N-terminal region alter the behavior of ORF1 phase separation. Removing the basic charged patch drastically reduces the ability of ORF1 to form droplets. Images were collected with noted concentration of ORF1$_{1\text{-}338}$ K3A/K4A/R7A/K8A at room temperature in 20 mM Tris pH 8.0, 1 mM DTT with NaCl concentration listed.

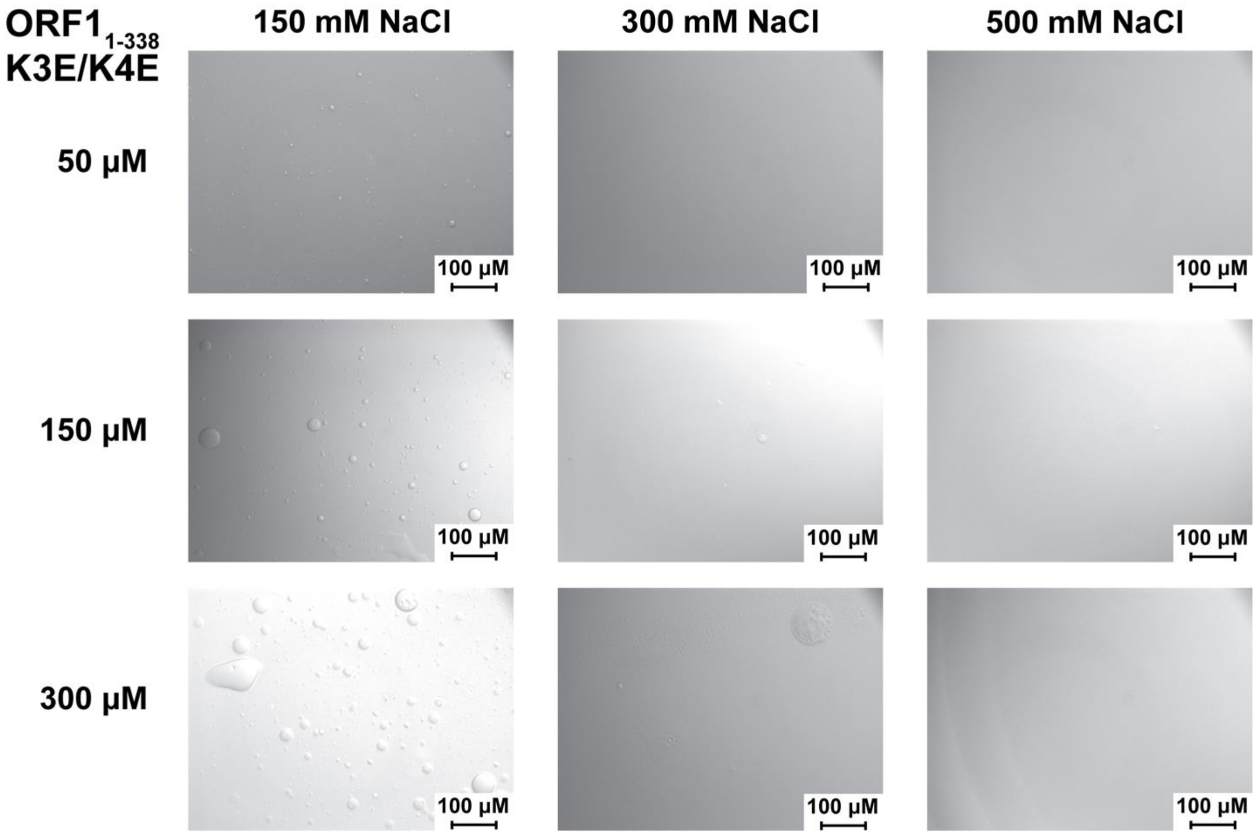

Figure S22. Phase separation of ORF1$_{1\text{-}338}$ K3E/K4E.
Mutations in the disordered N-terminal region alter the behavior of ORF1 phase separation. Exchanging the basic residues for acidic residues in the N-terminus reduces phase separation. Images were collected with noted concentration of ORF1$_{1\text{-}338}$ K3E/K4E at room temperature in 20 mM Tris pH 8.0, 1 mM DTT with NaCl concentration listed.

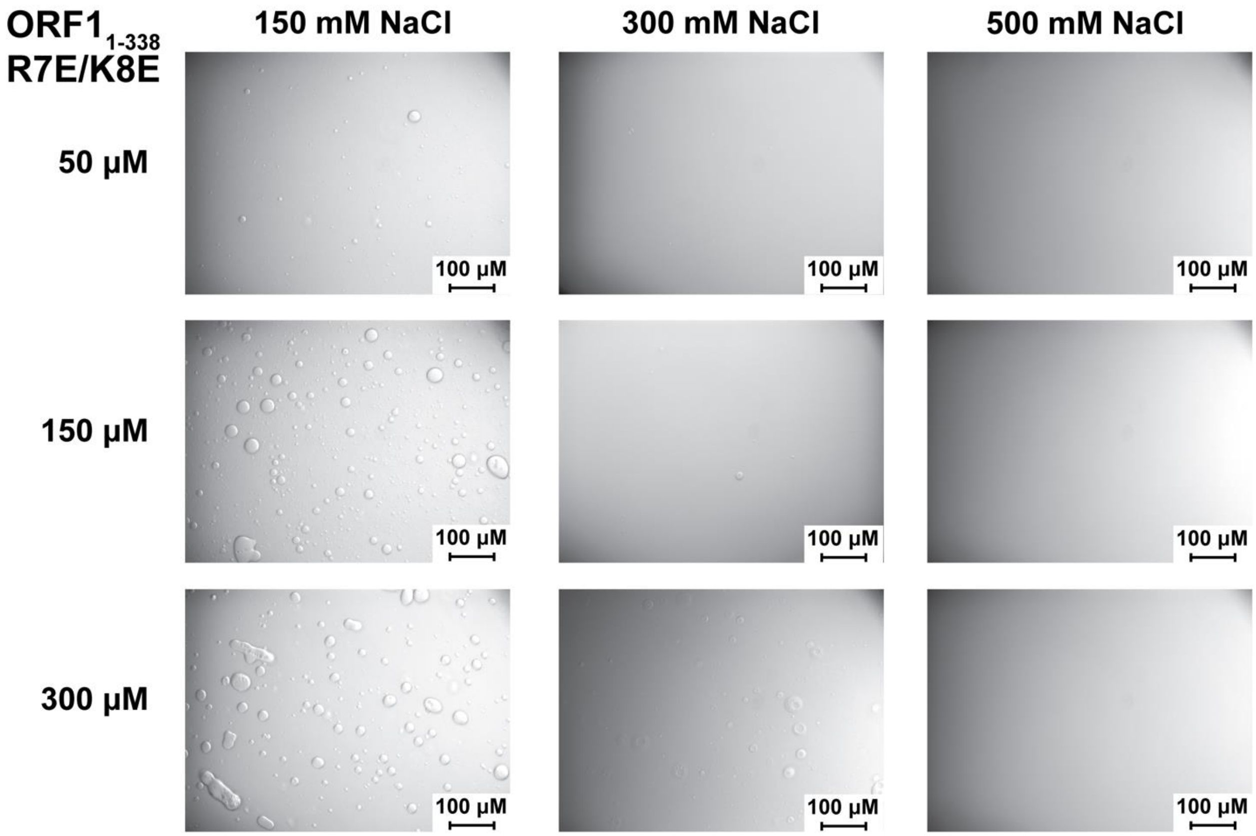

Figure S23. Phase separation of ORF1$_{1\text{-}338}$ R7E/K8E.
Mutations in the disordered N-terminal region alter the behavior of ORF1 phase separation. Exchanging the basic residues for acidic residues in the N-terminus reduces phase separation. Images were collected with noted concentration of ORF1$_{1\text{-}338}$ R7E/K8E at room temperature in 20 mM Tris pH 8.0, 1 mM DTT with NaCl concentration listed.

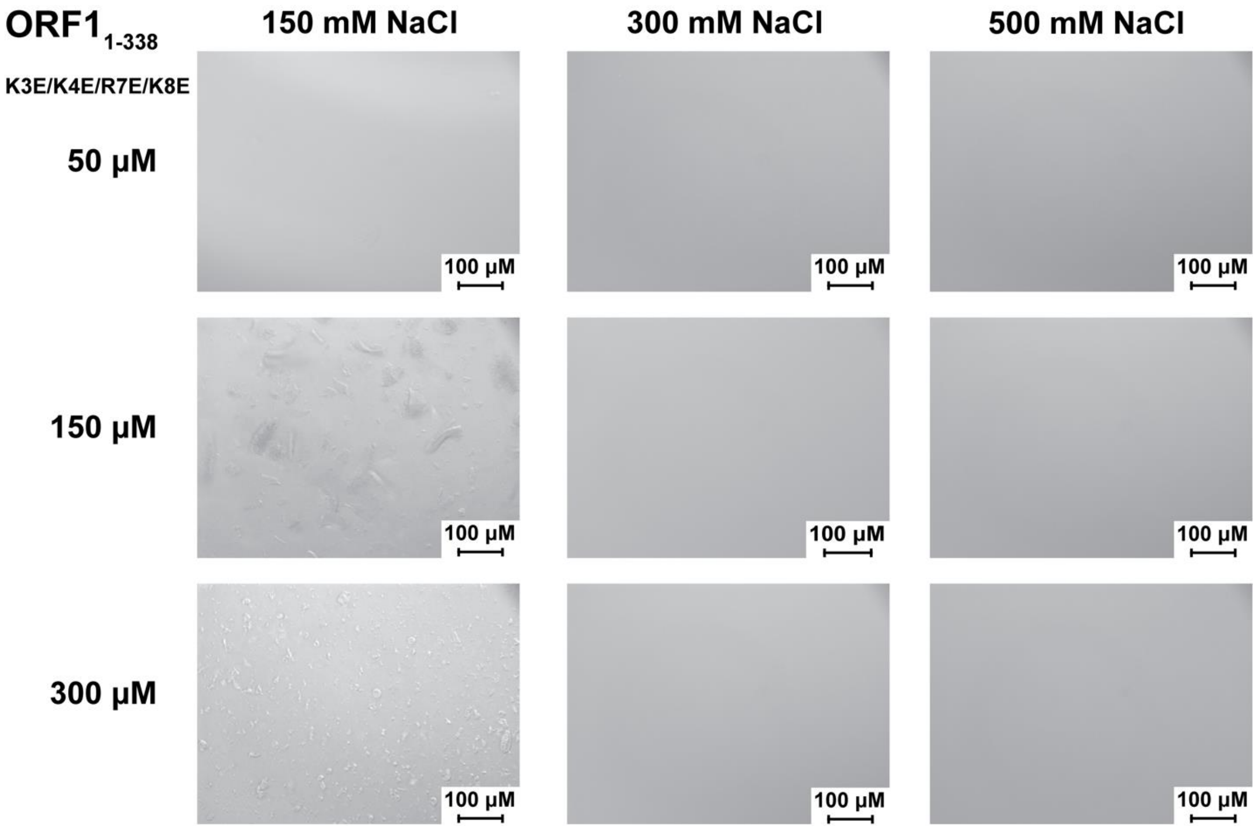

Figure S24. Phase separation of ORF1$_{1\text{-}338}$ K3E/K4E/R7E/K8E.
Mutations in the disordered N-terminal region alter the behavior of ORF1 phase separation. Exchanging all of the basic residues for acidic residues in the extreme N-terminus reduces phase separation and alters the morphology of the phase separated state at 150 mM NaCl. Images were collected with noted concentration ORF1$_{1\text{-}338}$ K3E/K4E/R7E/K8E at room temperature in 20 mM Tris pH 8.0, 1 mM DTT with NaCl concentration listed.

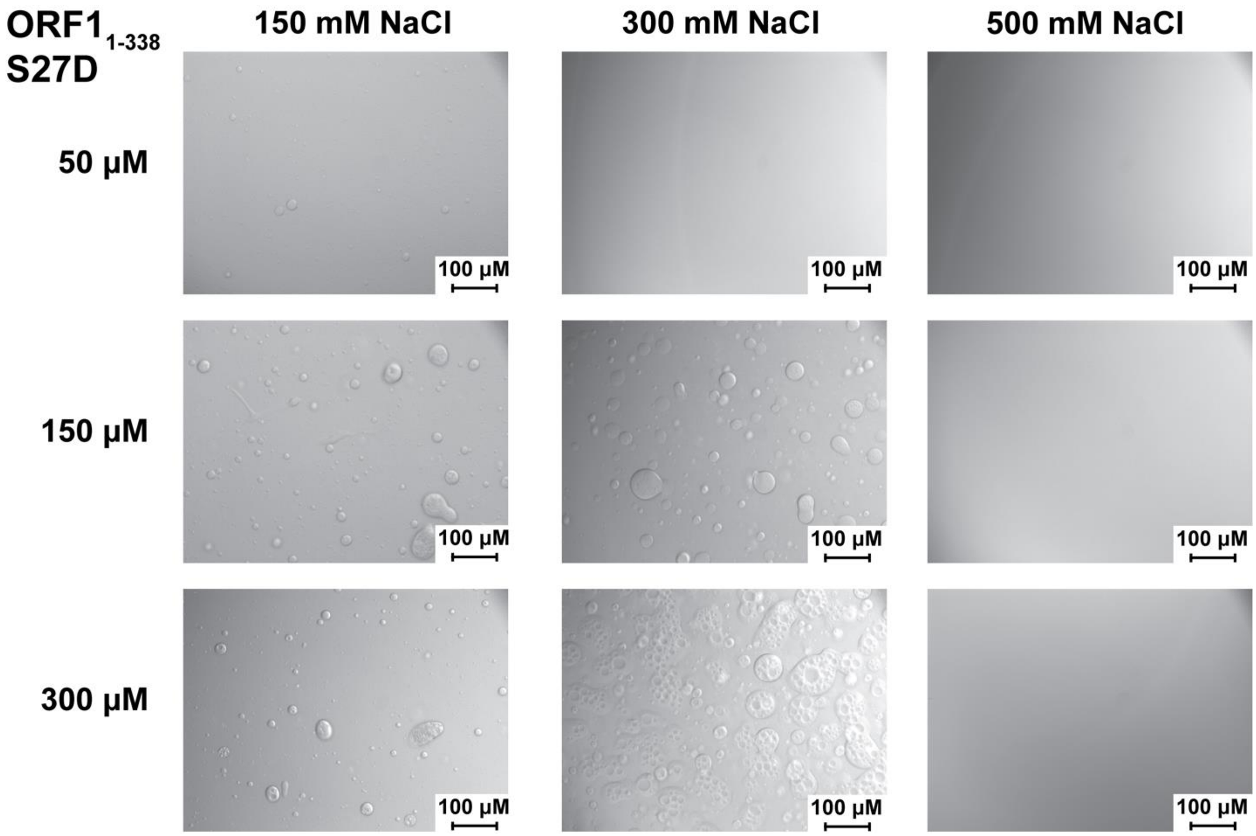

Figure S25. Phase separation of ORF1$_{1\text{-}338}$ S27D.
Mutations in the disordered N-terminal region alter the behavior of ORF1 phase separation. Introducing a phosphomimetic mutation at residue 27 increases phase separation and changes the droplet morphology at higher protein concentrations. Images were collected with noted concentration of ORF1$_{1\text{-}338}$ S27D at room temperature in 20 mM Tris pH 8.0, 1 mM DTT with NaCl concentration listed.

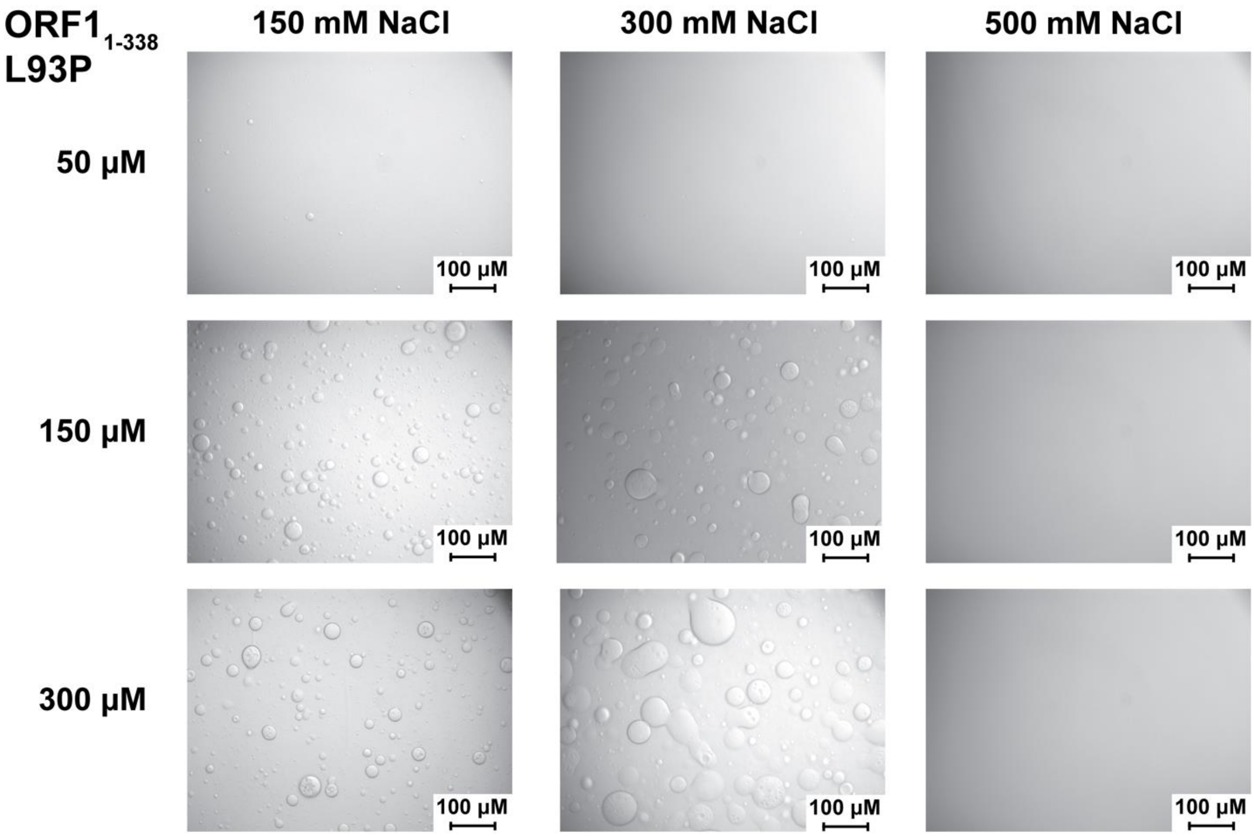

Figure S26. Phase separation of ORF1$_{1\text{-}338}$ L93P.
Mutations in the coiled-coil domain also affect the phase separation behavior of ORF1$_{1\text{-}338}$. Introducing a proline mutation at residue 93 in the stammer causes an increase in phase separation. Images were collected with noted concentration of ORF1$_{1\text{-}338}$ L93P at room temperature in 20 mM Tris pH 8.0, 1 mM DTT with NaCl concentration listed.

Supporting Reference

1. Penzkofer, T., M. Jager, M. Figlerowicz, R. Badge, S. Mundlos, P. N. Robinson, and T. Zemojtel. 2017. L1Base 2: more retrotransposition-active LINE-1s, more mammalian genomes. Nucleic Acids Res 45(D1):D68-D73.